HHS Public Access

Author manuscript

Brain Res. Author manuscript; available in PMC 2018 November 15.

Published in final edited form as:

Brain Res. 2017 November 15; 1675: 61–70. doi:10.1016/j.brainres.2017.09.007.

Chronic Global Analysis of Vascular Permeability and Cerebral Blood Flow after Bone Marrow Stromal Cell Treatment of Traumatic Brain Injury in the Rat : A long-term MRI Study

Lian Li[1], **Michael Chopp**[1,2], **Guangliang Ding**[1], **Qingjiang Li**[1], **Asim Mahmood**[3], and **Quan Jiang**[1]

[1]Department of Neurology, Henry Ford Health System, Detroit, MI 48202, USA

[2]Department of Physics, Oakland University, Rochester, MI 48309, USA

[3]Department of Neurosurgery, Henry Ford Health System, Detroit, MI 48208, USA

Abstract

Vascular permeability and hemodynamic alteration in response to the transplantation of human bone marrow stromal cells (hMSCs) after traumatic brain injury (TBI) were longitudinally investigated in non directly injured and normal-appearing cerebral tissue using magnetic resonance imaging (MRI). Male Wistar rats (300–350g, n=30) subjected to controlled cortical impact TBI were intravenously injected with 1 ml of saline (at 6-hours or 1-week post-injury, n=5/group) or with hMSCs in suspension (~3×10^6 hMSCs, at 6-hours or 1-week post-injury, n=10/group). MRI measurements of T2-weighted imaging, cerebral blood flow (CBF) and blood-to-brain transfer constant (Ki) of gadolinium-diethylenetriamine pentaacetic acid (Gd-DTPA), and neurological behavioral estimates were performed on all animals at multiple time points up to 3-months post-injury. Our long-term imaging data show that blood-brain barrier (BBB) breakdown and

Correspondence to: Quan Jiang.

	Author's Name	Telephone	E-mail
1	Lian Li (PhD)	313-916-2620	lli2@hfhs.org
2	Michael Chopp (PhD)	313-916-3936	MCHOPP1@hfhs.org
3	Guangliang Ding (PhD)	313-916-2620	gding1@hfhs.org
4	Qingjiang Li (MS)	313-916-2620	QLI1@hfhs.org
5	Asim Mahmood (MD)	313 916-1095	AMAHMOO2@hfhs.org
6	Quan Jiang (PhD)	313-916-8735	QJIANG1@hfhs.org

Mailing address for all authors: B126, Education & Research Building, Department of Neurology, Henry Ford Hospital, 2799 West Grand Boulevard, Detroit, MI 48202

Conflicts of interests

The authors have declared that no conflict of interest exists.

hemodynamic disruption after TBI, as revealed by Ki and CBF, respectively, affect both hemispheres of the brain in a diffuse manner. Our data reveal a sensitive vascular permeability and hemodynamic reaction in response to the time-dependent transplantation of hMSCs. A more rapid reduction of Ki following cell treatment is associated with a higher level of CBF in the injured brain, and acute (6h) cell administration leads to enhanced therapeutic effects on both the recovery of vascular integrity and stabilization of cerebral perfusion compared to delayed (1w) cell engraftment. Our results indicate that cell-enhanced BBB reconstitution plays an important role in underlying the restoration of CBF in the injured brain, which in turn, contributes to the improvement of functional outcome.

Keywords

Traumatic brain injury; Bone marrow stromal cells; Intervention; Vascular permeability; Cerebral blood flow; MRI

1. Introduction

Traumatic brain injury (TBI) is a serious public health problem worldwide and a major cause of mortality and morbidity in the young population (Rutland-Brown et al., 2006; Thurman et al., 1999). TBI not only produces primary insult, but also triggers a cascade of secondary pathologic events on the cellular and molecular levels, continuing to damage the brain. Despite extensive efforts over the past decades, no treatment is currently available that can effectively prevent or reverse the damage caused by secondary pathologies following TBI. Nevertheless, our understanding of the complex pathobiology of TBI has improved substantially. A number of factors that are involved in secondary brain injury have been identified, and increased cerebrovascular permeability and disturbed cerebrovascular perfusion by TBI are believed among the crucial ones (Chodobski et al., 2011; DeWitt and Prough, 2003; Shlosberg et al., 2010).

Experimental and clinical studies have shown that early blood-brain barrier (BBB) breakdown (Su et al., 2015; Tomkins et al., 2008; Yang et al., 2013) and hypoperfusion (Honda et al., 2016; Kaloostian et al., 2012; Kelly et al., 1997; Li et al., 2012; Stein et al., 2011; Ziegler et al., 2016) after TBI are associated with poor neurological outcome, indicating the detrimental role of BBB dysfunction and circulatory derangement in the pathophysiology of TBI. These vascular and hemodynamic abnormalities, which could last years following the trauma (Korn et al., 2005; Newsome et al., 2012; Tomkins et al., 2008), are not exclusively restricted within the ipsilateral hemisphere, but are heterogeneously present in both hemispheres of the injured brain (Beaumont et al., 2000; Dietrich et al., 1998; Hayward et al., 2011; Hendrich et al., 1999; Kim et al., 2010; Park et al., 2009; Pasco et al., 2007; Su et al., 2015), suggesting a dynamic pathophysiological evolvement in both time and space. Moreover, once these post-injury events are initiated, interaction between them may influence the ongoing brain damage (DeWitt and Prough, 2003; Fischer et al., 2002). The perturbed cerebral tissue perfusion may exacerbate the extent and duration of BBB opening by causing hypoxia of the cerebral tissue, while compromised vascular integrity contributes to cerebral edema and increased intracranial pressure, leading to

decreased blood flow in the injured brain (Dash et al., 2016; DeWitt and Prough, 2003; Fischer et al., 2002; Wei et al., 2012). The progression of these interplaying events after TBI in a broad area of brain, such as the entire cerebral tissue exclusive of the contusional lesion, may represent the brain response to the traumatic impact and provide insight into mechanisms of secondary brain injury. To the best of our knowledge, except for specific regional cerebral tissue analysis (Hayward et al., 2011; Kaloostian et al., 2012; Li et al., 2014; Long et al., 2015; Villapol et al., 2014; Wei et al., 2012), there have been no investigation of chronic global cerebral vascular response to TBI.

As the functional and pathological consequences of TBI, traumatic vascular injury and impaired hemodynamic homeostasis are attractive targets for therapeutic intervention (Chodobski et al., 2011; Kenney et al., 2016; Shlosberg et al., 2010; Thal and Neuhaus, 2014). Substantial data demonstrate that cell transplantation following TBI facilitates BBB reconstitution (Borlongan et al., 2004; Menge et al., 2012; Pati et al., 2011) and recovery of cerebral perfusion (Chen et al., 2013; Li et al., 2006; Li et al., 2011), which accompany therapeutic benefit on tissue repair (Li et al., 2011; Li et al., 2012). Dynamic changes in a widespread area of cerebral tissue may reflect the brain remodeling in response to the cell intervention. To date, however, most research has primarily focused on either BBB leakage (Su et al., 2015; Tomkins et al., 2008; Wei et al., 2012; Yang et al., 2013) or perfusion deficits (Chen et al., 2013; Honda et al., 2016; Kaloostian et al., 2012; Kelly et al., 1997). There are few studies (Li et al., 2016; Lin et al., 2012) documenting the dynamic relationship between the degree of BBB damage and perfusion status post-injury, especially within a long period of time post-TBI and in a broad area of cerebral tissue. Knowledge of these interactions may facilitate a better understanding of their roles in mediating cerebral injurious and restorative processes. Importantly, how the cell administration, a promising therapy known to attenuate secondary brain injury (Opydo-Chanek, 2007; Rolfe and Sun, 2015; Xiong et al., 2010) and enhance neurological performance (Jiang et al., 2011; Li et al., 2011; Tang et al., 2013), affects the evolution of BBB damage and tissue perfusion remains unclear. There is also a need to better elucidate the underlying mechanisms involved in cell-induced functional improvement after TBI. Treating TBI in the rat with human bone marrow stromal cells (hMSCs), we demonstrate that acute (e.g., 6 hours post-TBI) intravenous cell intervention exerts a potent therapeutic benefit in reducing cerebral atrophy, enhancing structural remodeling and improving neurological performance compared to delayed (e.g., 1 week post-TBI) intravenous cell administration (Li et al., 2011; Li et al., 2012; Li et al., 2017). However, whether this time-dependent therapeutic effect also modifies vascular and hemodynamic impairments is unknown. To address the above issues, the current study was conducted in a broad region of normal-appearing cerebral tissue identified on magnetic resonance imaging (MRI) to investigate a long-term and a global response of both vascular permeability and hemodynamic alteration in traumatic injured brain to the transplantation of hMSCs at 6 hours or 1 week post-TBI.

2. Results

All animals with saline injection (6h or 1w) post-TBI were considered as a saline-treated group, since no tendency towards statistical differences in MRI measurements and functional outcomes between the 6h–saline-treated and 1w–saline-treated group were found. Regarding

the dynamic changes of Ki and CBF after TBI, comparison between the ipsilateral and contralateral side of the injured brain was performed (Fig. 3 and Fig. 4). Investigation then focused on global response of the brain to the traumatic injury and intervention post-injury based on the evolution of Ki and CBF in the ROI (Fig. 1D) encompassing both hemispheres of normal-appearing cerebral brain tissue (Fig. 5). In the figures that present the temporal profiles of Ki and CBF after TBI either in separate hemispheres (Fig. 3 and Fig. 4) or in both hemispheres (Fig. 5), mean values of Ki and CBF obtained from pre-injured cerebral tissue for each group are illustrated as dotted lines.

2.1. Changes of Ki in two hemispheres of the brain after TBI

Dynamic changes of Ki in two sides of normal-appearing brain tissue with and without cell administration after TBI are shown in Fig. 3. A statistical difference in Ki between two sides of the brain was detected within 1-week after TBI for all three groups (Fig. 3A–3C), with significantly higher Ki values being present in the ipsilateral side than in the contralateral side of the injured brain. After 1-week post-TBI, similar temporal profiles of Ki were present in both cerebral hemispheres for each group without statistical difference, even though each group with (Fig. 3A–3B) or without (Fig. 3C) cell intervention exhibited its own temporal pattern of Ki.

2.2. Changes of CBF in two hemispheres of the brain after TBI

As shown in Fig. 4, the situation of CBF varying in the two cerebral hemispheres of normal-appearing brain tissue along with time after TBI resembled that of Ki. A statistical difference in CBF between two sides of the brain was only found at 1-day after TBI for all groups (Fig. 4A–4C), with significantly higher CBF values being detected in the ipsilateral side than in the contralateral side of the injured brain. Thereafter, there was no statistical difference in CBF between two sides of the brain for each group, even though distinctive features were observed in the temporal profile of CBF for the saline and cell treatment groups.

2.3. Therapeutic effects of cell engraftment on Ki and CBF in the injured brain

The temporal profiles of Ki (Fig. 5A) and CBF (Fig. 5B) post-TBI obtained from ROI (Fig. 1) encompassing both sides of normal-appearing brain tissue are shown in Fig. 5, representing the global response of the brain to the traumatic injury and cell intervention post-injury.

A general three-stage temporal profile pattern of Ki post-TBI for all groups is presented in Fig. 5A, with TBI-induced elevated Ki persisting for about 3-weeks (stage 1), followed by a rapid decrease in Ki between 3-weeks and 2-months (stage 2) and a reduced variation in Ki after 2-months (stage 3). Along with time after TBI, significant Ki reduction was detected for each treatment group between the first (3-weeks) and last (2-months) time point in stage 2, while no such alteration in Ki was found for each group in stage 1 and 3. Compared to the saline-treated group, cell administration expedited Ki reduction in stage 2 and led to lower Ki values in stage 3.

The corresponding temporal profiles of CBF for all groups are shown in Fig. 5B. These data also reveal a fundamental three-stage development of CBF along with time after TBI, characterized by a pronounced change in stage 2 and a relatively slight fluctuation in stage 1 and 3 for each treatment group. However, significant CBF reduction between the first (3-weeks) and last (2-months) time point in stage 2 was only detected in the saline-treated and 1w–cell-treated group, not in the 6h–cell-treated group. By effectively retarding the decrease of CBF in stage 2, acute (6h) cell intervention after TBI retains the higher CBF values in stage 3 than do saline and delayed cell administration.

There is no statistical difference in both Ki and CBF among the experimental groups within stages 1 and 2 until the beginning of stage 3. Acute cell treatment following TBI results in significantly reduced Ki (at 2-months and 3-months, cell-6h vs. control, $p < 0.05$) and elevated CBF (at 2-months, cell-6h vs. control, $p < 0.05$) values in stage 3 compared to saline treatment.

2.4. Lesion volume and functional outcome

There was no difference in lesion volume among the treatment groups (cell or saline intervention) during the observation period (Fig. 6A). An improved functional performance, as measured by water maze test, was detected in the cell-treated groups compared to the saline-treated group (Fig. 6B). The cell-treated animals spent significantly longer time in the correct quadrant than the saline-treated animals and this enhanced status remains throughout the observation period. However, no group difference between acute and delayed cell administration was found.

3. Discussion

In a broad region of normal-appearing cerebral tissue, vascular permeability and hemodynamic alteration in response to the transplantation of hMSCs after TBI were longitudinally investigated up to 3-months post-injury. Our long-term imaging data show that BBB breakdown and hemodynamic disruption after TBI, as revealed by Ki and CBF, respectively, affect both hemispheres of the brain in a diffuse manner. Treatment with hMSCs after TBI expedites the reduction of Ki which is associated with the increased level of CBF in the injured brain. Compared to delayed (1w) cell transplantation, acute (6h) cell administration results in a more rapid recovery of vascular integrity and a stronger restoration of cerebral perfusion, indicating a strategy-dependent (e.g., the timing of cell transplantation) therapeutic effect and a positive hemodynamic response to BBB reconstitution.

BBB is the regulated interface between the peripheral blood circulation and the central nervous system, and plays a vital role in creating a highly stable biochemical environment in the brain for the normal functioning of neuronal cells (Beaumont et al., 2000; Chodobski et al., 2011; Shlosberg et al., 2010). Brain imaging data from both animal models and patients with TBI confirms the high incidence of BBB damage after TBI (Korn et al., 2005; Su et al., 2015; Tomkins et al., 2008). By potentially allowing the circulating immune cells and blood-borne substances into the brain, BBB disruption may add to the initial insult in the setting of brain injury, leading to augmented inflammatory response, edema formation and further

neuronal damage (Shlosberg et al., 2010). Adequate cerebral perfusion is essential for healthy brain function. Cerebral blood flow is tightly regulated to meet the brain's metabolic demands. This hemodynamic homeostasis, however, is often compromised post-TBI, resulting in hypoperfusion and ischemic tissue damage (Prabhakar et al., 2014). To understand how these vascular and hemodynamic alterations post-TBI are involved in and possibly mediate cerebral injurious processes, extensive studies have been performed with a great attention paid to regional analysis (Hayward et al., 2011; Kaloostian et al., 2012; Li et al., 2014; Long et al., 2015; Villapol et al., 2014; Wei et al., 2012). Nevertheless, growing evidence indicates that BBB breakdown and hypoperfusion, the important secondary pathophysiologic consequences of TBI present chronically in the injured brain (Korn et al., 2005; Newsome et al., 2012; Tomkins et al., 2008), are not regional events, even though the primary initiating injury may be a focal impact. These post-injury abnormalities occur and affect the brain heterogeneously and globally (Beaumont et al., 2000; Dietrich et al., 1998; Hayward et al., 2011; Hendrich et al., 1999; Kim et al., 2010; Park et al., 2009; Pasco et al., 2007; Su et al., 2015). It has also been reported that intravenously delivered hMSCs after TBI lead to a widespread spatial modification of hemodynamic and structural impairments in the traumatized brain, despite the high concentration of the grafted cells around the contusional lesion compared to other areas in the brain (Li et al., 2011; Li et al., 2012; Mahmood et al., 2003). Based on these findings, we therefore conducted our long-term investigation in a broad region of normal-appearing cerebral tissue identified on MRI, where impact-induced damage (Pasco et al., 2007; Sidaros et al., 2009; Su et al., 2015; Wang et al., 2008) and post-injury remodeling by either spontaneous or treatment-derived action (Li et al., 2011; Li et al., 2012; Li et al., 2017) are taking place with time after TBI.

Local injury in the brain is associated with distal diaschisis, occurring in non directly injured brain regions remote from but neuroanatomically connected to the site of initial insult (Carrera and Tononi, 2014). The physiological changes in diaschisis, present not only in the ipsilateral but also in the contralateral brain hemisphere, include compromised BBB integrity (Garbuzova-Davis et al., 2013; Garbuzova-Davis et al., 2014) plus corresponding edema (Izumi et al., 2002), hypoperfusion and hypometabolism (Carrera and Tononi, 2014). By improving blood flow and metabolism in both hemispheres of ischemia-injured brain, cell therapy has been shown to facilitate the normalization of diaschisis-associated physiological changes, particularly at the level of cerebral vasculature (Taguchi et al., 2015). Our data confirm the observations (Beaumont et al., 2000; Dietrich et al., 1998; Hayward et al., 2011; Hendrich et al., 1999; Kim et al., 2010; Park et al., 2015; Pasco et al., 2007; Su et al., 2015) that an unilateral focal impact leads to BBB opening and hemodynamic alteration, as detected by Ki and CBF, which spread into the remote brain areas both ipsilateral and contralateral to the primary injury (Carrera and Tononi, 2014; Taguchi et al., 2015). Within an initial short period (less than 1-week) post-injury, a difference in the degree of traumatic injury influence on Ki and CBF between the two hemispheres was found regardless of intervention (cell or saline) and cell treatment strategy (6h or 1-week), with significantly more severe effects present in the ipsilateral-side than in the contralateral-side of the brain (Fig. 3 and Fig. 4). These data demonstrate that our severe CCI-TBI model induces a large difference in acute pathologic response between two hemispheres. The observed hyperperfusion in the ipsilateral hemisphere and hypoperfusion in the contralateral

hemisphere may represent a compensatory physiologic mechanism after unilateral trauma and the possible involvement of neovascularization evoked by the injury (Park et al., 2009). After 1-week, however, similar injury status in the two hemispheres characterized by Ki and CBF was observed, suggesting that focal trauma eventually results in pathological alterations throughout the brain, and that cell transplantation influences both hemispheres of the injured brain. These findings are consistent with the previous observation that TBI affects the brain diffusely, and cell engraftment exerts modulatory effects over a considerable spatial extent (Aertker et al., 2015; Dori et al., 2016; Li et al., 2011; Li et al., 2012; Taguchi et al., 2015). Our data also reveal that compared to un-injured brain (dotted lines in Fig. 3 and Fig. 4), increased Ki and decreased CBF in both brain hemispheres persist to 3-months in the injured brain (Fig. 3C, Fig. 4C), while cell intervention, especially acute cell administration (Fig. 3A and Fig. 4A), ameliorates these injury-induced vascular and hemodynamic abnormalities with time after TBI. These physiological alterations in response to the treatments (saline or cell) support the idea of chronic diaschisis (Garbuzova-Davis et al., 2014) and the therapeutic action of cell therapy on cerebral vasculature (Taguchi et al., 2015).

Data from ROI (Fig. 1D) encompassing both hemispheres show that temporal profiles of Ki and CBF for all groups with or without cell intervention exhibit a general three-stage evolution pattern (Fig. 5), with TBI-induced initial disturbance of Ki and CBF lasting for about 3-weeks (stage 1), followed by a dramatic change in Ki and CBF between 3-weeks and 2-months (stage 2), and a reduced variation of these parameters after 2-months (stage 3). It is worth noting that the dynamic temporal evolution of Ki nicely corresponds with that of CBF stage by stage (compare Fig. 5A with 5B), such as fluctuating in stage 1, reduced in stage 2, and tending towards stability in stage 3, representing a close relationship between vascular injury and hemodynamic disruption post-TBI. Considering the profiles presented by control group, the feature of staged evolution of Ki and CBF is consistent with previous findings. As revealed by the vast majority of investigations, BBB breakdown and hemodynamic disruption rapidly occur and persist in the early phase after TBI, with heterogeneously disturbed Ki and CBF detected in the injured brain both temporally and spatially (Engel et al., 2008; Li et al., 2016; Lin et al., 2012; Long et al., 2015; Su et al., 2015). Although gradually reversal of these pathologic changes are regionally observed in the follow-up period of time (such as 1-month post-TBI) (Villapol et al., 2014; Wei et al., 2012), compromised BBB integrity (Korn et al., 2005; Tomkins et al., 2008) as well as widespread hypoperfusion beyond the contusional lesion (including hippocampus, thalamus and perilesional regions) (Hayward et al., 2010; Liu et al., 2013) chronically persist. The profiles also illustrate that for each treatment group, the pronounced change of both Ki and CBF takes place in stage 2, largely determining the subsequent levels of these measures in stage 3. By expediting the reduction of Ki and retarding the diminution of CBF, transplantation of hMSCs post-TBI alters the Ki and CBF profiles in opposite directions in stage 2, leading to lower Ki and higher CBF values in stage 3 compared to saline administration. Most importantly, we detected a sensitive hemodynamic reaction to the status of vascular permeability in response to the transplantation of hMSCs. As shown in Fig. 5, acute cell engraftment results in a large decrease of Ki, starting from stage 2 and continuing to stage 3, which is associated with a notable rescue of CBF, while these

therapeutic effects induced by delayed cell intervention on both Ki and CBF are less potent. Moreover, our data present evidence that a more rapid recovery of vascular integrity, as a result of cell engraftment, occurs in parallel with a stronger restoration of cerebral perfusion and a better neurological performance (compare Fig. 5A–5B with Fig. 6B), supporting the concept that BBB integrity is critical for maintaining brain homeostasis and function (Beaumont et al., 2000; Chodobski et al., 2011; Shlosberg et al., 2010). These results suggest that enhanced BBB integrity induced with cell administration contributes to stabilization of cerebral perfusion, and hence neural recovery.

The underlying mechanisms accounting for protective action of MSCs on BBB are multifactorial, including modulation of astrocytic endfeet and VEGF-A signaling (Park et al., 2015), suppression of inflammatory cytokines (Tang et al., 2014) and reduction of astrocyte apoptosis (Tang et al., 2014). Our longitudinal data (Fig. 5) demonstrate that the therapeutic effect of acute cell intervention on amelioration of vascular deficit associated with TBI is greater than that of delayed cell administration, indicating the importance of timing of transplantation in cell therapy. Previous reports suggest that the grafted MSCs in the injured brain serve as *in vivo* local source of cytokines and trophic factors that activate endogenous restorative and regenerative processes (Chopp and Li, 2006; Parr et al., 2007), while recent investigations indicate that MSCs could also exert a systemic effect through the secretion of soluble factors that act in a global manner (Chen et al., 2015; Lee et al., 2009; Menge et al., 2012; Pati et al., 2011). In support of this premise, potent therapeutic benefits of MSCs on cerebral tissue repair have been observed without significant engraftment in the brain (Li et al., 2011; Li et al., 2012; Li et al., 2017; Mahmood et al., 2003). Since these soluble factors are systemically released by activated MSCs once intravenously infused, their influence may rely on the time when the intervention starts, instead of when the cells migrate into the brain. Therefore, the enhanced effect of hMSCs on BBB reconstitution observed in the current study resulting from acute cell intervention compared to delayed cell administration may be at least explained in part by an earlier initiated global action of soluble factors released from hMSCs in attenuating the inflammatory response (Chen et al., 2015; Haus et al., 2016; Menge et al., 2012) which may inhibit compromise of the BBB (Menge et al., 2012).

In agreement with the previous findings (Haus et al., 2016; Li et al., 2011; Li et al., 2012; Li et al., 2017), our long-term measurements demonstrate the significant improvement of neurological performance after transplantation of hMSCs (Fig. 6B) without lesion reduction (Fig. 6A), suggesting that improved functional recovery is attributed to cell-enhanced brain remodeling (Haus et al., 2016; Li et al., 2011; Li et al., 2012; Li et al., 2017), including neurovascular restoration, in the normal-appearing tissue region. No difference in mMWM performance between acute and delayed cell intervention may possibly be attributed to the similar effect of cell-enhanced hippocampal neuronal survival provided by the two treatment strategies (Xiong et al., 2009).

In summary, we demonstrate a three-stage temporal profile of both Ki and CBF post-TBI in normal-appearing cerebral region. Stage by stage, these related indices also exhibit a corresponding response to the traumatic injury and cell intervention, indicative of a close relationship between vascular damage and perfusion disturbance after TBI. Our data reveal a

sensitive hemodynamic reaction to the status of vascular permeability in response to the transplantation of hMSCs, and a strategy-dependent treatment result. A more rapid reduction of Ki following cell treatment is associated with a higher level of CBF in the injured brain, and acute cell administration leads to more effective therapeutic effects on both the recovery of vascular integrity and stabilization of cerebral perfusion compared to delayed cell engraftment. The findings of the current study indicate that cell-enhanced BBB reconstitution plays an important role underlying the CBF restoration in the injured brain, which in turn, contributes to the improvement of functional outcome.

4. Experimental procedures

All experimental procedures were conducted in accordance with the NIH Guide for the Care and Use of Laboratory Animals and approved by the Institutional Animal Care and Use Committee (IACUC#1316) of Henry Ford Health System.

4.1. Animal model and experimental groups

The controlled cortical impact (CCI) TBI animal model has been previously described (Li et al., 2011; Li et al., 2012). Briefly, male Wistar rats (300 to 350g, n = 30) were anesthetized with chloral hydrate (350 mg/kg, i.p.) and their rectal temperature was maintained at 37°C with a feedback-regulated water-heating pad. The head of each animal was mounted in a stereotactic frame and two 10-mm-diameter craniotomies, one in each hemisphere, were performed adjacent to the central suture, midway between the lambda and the bregma, with special attention being paid to leave the dura mater over the cortex intact. The left craniotomy confined the location of experimental impact, while the right one allowed for the lateral movement of cortical tissue. Using a CCI device, a unilateral brain injury was induced by delivering a single impact at a velocity of 4 m/sec reaching a depth of 2.5 mm below the dura mater layer to the left cortex with a pneumatic piston containing a 6-mm-diameter tip. The injury induced by this CCI model affects the primary motor and somatosensory cortex, and the underlying hippocampus. Following the operation, the bone flap was replaced and sealed with bone wax, and the skin was sutured. For analgesia, Buprenex (0.05 mg/kg, s.q.) was administered to each animal after brain injury.

The hMSCs were purchased from Theradigm (Baltimore, MD). The cells were suspended in phosphate-buffered saline (PBS) prior to injection into rats, which was performed at 6 hours or 1 week post-TBI. Rats subjected to brain injury were randomized to one of four treatment groups, 6h–cell-treated (n = 10), 1w–cell-treated (n = 10), 6h–saline-treated (n = 5) and 1w–saline-treated (n = 5) groups. Anesthesia was reinstituted before the transplantation and a bolus of the cell suspension (~ 3×10^6 hMSCs in 1 ml PBS) was slowly infused over a 5-minute period into the tail vein of each rat in the cell-treated groups using a Hamilton syringe. The needle was left in place for 1 minute before withdrawal to minimize cell leakage, and the injection site was compressed for a short time to reduce bleeding. Replacing the cell suspension with the same amount of saline, each animal in the saline-treated groups underwent the identical procedures as those in the cell-treated groups.

4.2. MR imaging and data processing

MR imaging was performed using ClinScan 7T system (Siemens, Erlanger, Germany). The animal was securely fixed on a MR-compatible holder equipped with an adjustable nose cone for administration of anesthetic gases and stereotaxic ear bars to immobilize the head. For reproducible positioning of the animal in the magnet, a fast gradient echo imaging sequence was used at the beginning of each MRI session. During image acquisition, anesthesia was maintained by a gas mixture of 1.0% – 1.5% isoflurane in medical air (1.0L/min), and rectal temperature was kept at 37±1.0°C using a feedback-controlled water bath (YSI Inc, Yellow Springs, OH) underneath the animal. T2-weighted imaging (T2WI), cerebral blood flow (CBF) and blood-to-brain transfer constant (Ki) of gadolinium-diethylenetriamine pentaacetic acid (Gd-DTPA) were repeatedly acquired for all animals at multiple time points up to 3 months following TBI (1 day pre-TBI, 1 day post-TBI, weekly afterwards for 3 weeks, then 5 weeks, 2 months and 3 months). All rats were killed after the final *in vivo* MRI scans.

T2WI was acquired using a multi-slice (13 slices, 1 mm thick), multi-echo (6 echoes) sequence with echo times (TE) of 15, 30, 45, 60, 75 and 90 ms, and a repetition time (TR) of 4.5 s. Images were produced with a 32 × 32 mm^2 field of view (FOV) and a 128 × 64 image matrix. T2 maps were calculated on a voxel-wise basis by linear least-squares fit of the logarithm of the signal intensity versus TE (Eigentool image analysis software, Henry Ford Health System, MI, USA),

To measure the Ki, the dynamic contrast-enhanced MRI (DCE-MRI) was performed with a dual gradient echo (DGE) sequence (Ewing and Bagher-Ebadian, 2013; Yu et al., 2010). The total scan time was approximately 5 minutes by repeating the DGE sequence 150 times (TE of 1.5 ms and 8 ms, TR of 33 ms, 3 slices, 2 mm thick, 32 × 32 mm FOV, 128 × 64 image matrix). After a baseline scan of 15 seconds (~ 10 sets of serial images), a bolus of Gd-DTPA (0.2 mmol/kg) was manually delivered within 5 seconds via tail vein while the rest of the scan was continuously going on. To produce pre-contrast T1 map, a variable flip angle spoiled gradient-echo approach was employed with TE of 4 ms, TR of 30 ms, 8 slices, 2 mm thick and flip-angles of 2°, 5°, 10°, 15°, 20° and 25°. Under the assumption that a change in 1/T1 (ΔRl(t)) is linearly proportional to a change in both plasma (Cpa(t)) and tissue (Ctis(t)) concentrations of contrast agent and the assumption that the constant of proportionality is the same for tissue and blood, ΔR1(t)s measured in tissue (ΔR1tis(t)) and sagittal sinus (ΔR1pa(t)) were used as estimates of Ctis(t) and Cpa(t), respectively. Using Patlak plots (Ewing et al., 2003), linear least-squares estimates of slope (Ki) were determined for each pixel and maps of Ki were constructed.

Cerebral blood flow (CBF) was estimated using a pulsed arterial spin labeling (PASL) technique, known as quantitative imaging of perfusion using a single subtraction, second version (QUIPSS II) with thin slice TI1 periodic saturation (Q2TIPS) and applying the proximal inversion with a control for off resonance effects (PICORE) labeling scheme (Luh et al., 1999; Wong et al., 1997; Wong et al., 1998). Single-shot of echo-planar readout was used for each 2 mm slice (total 5 slices) perpendicular to the magnetic field direction. PASL imaging parameters were: 32 × 32 mm^2 FOV, 128 × 128 image matrix, TR of 3000 ms, TE of 18 ms, inversion time of 1000 ms. Bipolar crusher gradients were applied with a cutoff

speed of 60 cm/s. The 80 mm labeling slab was positioned with a 6.1 mm gap caudal to the imaging slab.

A representative slice of T2, Ki and CBF maps is shown in Fig. 1, where TBI-induced disturbance was apparent around the impact site on each map (Fig. 1A–1C). With a sensitivity to the abnormalities and a capacity to reveal the anatomical information of the brain, T2 map was selected for delineating the region of interest (ROI). As shown in Fig. 1A, ventricles and TBI-affected cerebral cortex were present as hyperintense regions on T2 map. To create the ROI encompassing the normal-appearing cerebral tissue without contamination of these regions (Fig. 1D, red track), a threshold value (mean+2s.d. measured from the cerebral tissue) (Li et al., 2011; Li et al., 2012) provided by pre-injured brain scan was used. To examine the effect of unilateral injury on different sides of the brain, the ROI was divided to two parts (Fig. 1D, green line), impact side and contralateral side (Fig. 1D, indicated by green arrows). Longitudinal evaluation of Ki and CBF was performed within the ROI as well as within the two parts of the ROI (Eigentool image analysis software, Henry Ford Health System, MI, USA). With the series of T2, Ki and CBF maps, Fig. 2 shows a dynamic comparison of representative animals with (Fig. 2A) and without (Fig. 2B) cell intervention post-injury and a typical lesion in the injured brain (Fig. 2C).

4.3. Modified Morris water maze test (mMWM)

To evaluate the long-term functional outcome of spatial learning acquisition and memory retention, the mMWM (Mahmood et al., 2007; Mahmood et al., 2011) was used. The testing system consisted of a circular tank (180cm in diameter and 45cm high) filled with 30°C water and a hidden-platform (15cm in diameter and 35cm high) set inside the tank 1.5cm below the surface of the water. The pool was located in a large test room decorated with visual clues (for example, pictures, lamps and so forth) that remained constant during the study and enabled the rats to orientate themselves spatially. For descriptive data collection, an automated tracking system (HVS Image, San Diego, CA, USA) was employed and the pool was subdivided into four equal quadrants formed by imaging lines.

The rats were tested on 5 consecutive days at the last week of study period (from day 85 to 89 after TBI). Each trial was initiated by placing the animal randomly at one of four start locations (North, South, East and West) and allowing 90s to find the hidden platform. The platform was put in a randomly changing position within the northeast (NE) quadrant throughout the test period (e.g., sometimes equidistant from the center and edge of the pool, against the wall, near the center of the pool, and at the edges of the NE quadrant). After locating the platform, the animal was allowed to remain on the platform for 15s before being returned to its cage. If the animal failed to find the platform within 90s, the experiment was terminated and a maximum score of 90s was assigned. The percentage of time traveled within the NE (correct) quadrant was calculated relative to the total amount of time spent swimming before reaching the platform. The advantage of this modified version of the water maze is that with the platform being relocated randomly within the target quadrant, each trial effectively acts as a probe trial.

4.4. Statistical analysis

Analysis of covariance (ANCOVA) was employed to compare the group difference in MRI measurements (Ki, CBF and lesion volume) and functional assessments (mMWM) with the independent factor of treatment and dependent factor of time. Analysis began with testing the treatment group and time interaction, followed by testing the group difference at each time point and the time effect for each treatment group if the interaction or the overall group/time effect was detected at the 0.05 level. A subgroup analysis would be considered if the interaction or main effect of group/time was not at the 0.05 level. Results are presented as mean ± standard error (SE). Statistical significance was inferred for $p \leq 0.05$.

Acknowledgments

We thank Dr. Changsheng Qu for animal experiment assistance. This work was supported by National Institutes of Health RO1 NS064134.

References

Aertker BM, Bedi S, Cox CS Jr. Strategies for CNS repair following TBI. Exp Neurol. 2015

Beaumont A, Marmarou A, Hayasaki K, Barzo P, Fatouros P, Corwin F, Marmarou C, Dunbar J. The permissive nature of blood brain barrier (BBB) opening in edema formation following traumatic brain injury. Acta Neurochir Suppl. 2000; 76:125–9. [PubMed: 11449990]

Borlongan CV, Lind JG, Dillon-Carter O, Yu G, Hadman M, Cheng C, Carroll J, Hess DC. Intracerebral xenografts of mouse bone marrow cells in adult rats facilitate restoration of cerebral blood flow and blood-brain barrier. Brain Res. 2004; 1009:26–33. [PubMed: 15120580]

Carrera E, Tononi G. Diaschisis: past, present, future. Brain. 2014; 137:2408–22. [PubMed: 24871646]

Chen M, Li X, Zhang X, He X, Lai L, Liu Y, Zhu G, Li W, Li H, Fang Q, Wang Z, Duan C. The inhibitory effect of mesenchymal stem cell on blood-brain barrier disruption following intracerebral hemorrhage in rats: contribution of TSG-6. J Neuroinflammation. 2015; 12:61. [PubMed: 25890011]

Chen X, Yin J, Wu X, Li R, Fang J, Chen R, Zhang B, Zhang W. Effects of magnetically labeled exogenous endothelial progenitor cells on cerebral blood perfusion and microvasculature alterations after traumatic brain injury in rat model. Acta Radiol. 2013; 54:313–23. [PubMed: 23528570]

Chodobski A, Zink BJ, Szmydynger-Chodobska J. Blood-brain barrier pathophysiology in traumatic brain injury. Transl Stroke Res. 2011; 2:492–516. [PubMed: 22299022]

Chopp M, Li Y. Transplantation of bone marrow stromal cells for treatment of central nervous system diseases. Adv Exp Med Biol. 2006; 585:49–64. [PubMed: 17120776]

Dash PK, Zhao J, Kobori N, Redell JB, Hylin MJ, Hood KN, Moore AN. Activation of Alpha 7 Cholinergic Nicotinic Receptors Reduce Blood-Brain Barrier Permeability following Experimental Traumatic Brain Injury. J Neurosci. 2016; 36:2809–18. [PubMed: 26937017]

DeWitt DS, Prough DS. Traumatic cerebral vascular injury: the effects of concussive brain injury on the cerebral vasculature. J Neurotrauma. 2003; 20:795–825. [PubMed: 14577860]

Dietrich WD, Alonso O, Busto R, Prado R, Zhao W, Dewanjee MK, Ginsberg MD. Posttraumatic cerebral ischemia after fluid percussion brain injury: an autoradiographic and histopathological study in rats. Neurosurgery. 1998; 43:585–93. discussion 593–4. [PubMed: 9733314]

Dori I, Petrakis S, Giannakopoulou A, Bekiari C, Grivas I, Siska EK, Koliakos G, Papadopoulos GC. Seven days post-injury fate and effects of genetically labelled adipose-derived mesenchymal cells on a rat traumatic brain injury experimental model. Histol Histopathol. 2016; 11864

Engel DC, Mies G, Terpolilli NA, Trabold R, Loch A, De Zeeuw CI, Weber JT, Maas AI, Plesnila N. Changes of cerebral blood flow during the secondary expansion of a cortical contusion assessed by 14C–iodoantipyrine autoradiography in mice using a non-invasive protocol. J Neurotrauma. 2008; 25:739–53. [PubMed: 18627253]

Ewing JR, Knight RA, Nagaraja TN, Yee JS, Nagesh V, Whitton PA, Li L, Fenstermacher JD. Patlak plots of Gd-DTPA MRI data yield blood-brain transfer constants concordant with those of 14C–sucrose in areas of blood-brain opening. Magn Reson Med. 2003; 50:283–92. [PubMed: 12876704]

Ewing JR, Bagher-Ebadian H. Model selection in measures of vascular parameters using dynamic contrast-enhanced MRI: experimental and clinical applications. NMR Biomed. 2013; 26:1028–41. [PubMed: 23881857]

Fischer S, Wobben M, Marti HH, Renz D, Schaper W. Hypoxia-induced hyperpermeability in brain microvessel endothelial cells involves VEGF-mediated changes in the expression of zonula occludens-1. Microvasc Res. 2002; 63:70–80. [PubMed: 11749074]

Garbuzova-Davis S, Rodrigues MC, Hernandez-Ontiveros DG, Tajiri N, Frisina-Deyo A, Boffeli SM, Abraham JV, Pabon M, Wagner A, Ishikawa H, Shinozuka K, Haller E, Sanberg PR, Kaneko Y, Borlongan CV. Blood-brain barrier alterations provide evidence of subacute diaschisis in an ischemic stroke rat model. PLoS One. 2013; 8:e63553. [PubMed: 23675488]

Garbuzova-Davis S, Haller E, Williams SN, Haim ED, Tajiri N, Hernandez-Ontiveros DG, Frisina-Deyo A, Boffeli SM, Sanberg PR, Borlongan CV. Compromised blood-brain barrier competence in remote brain areas in ischemic stroke rats at the chronic stage. J Comp Neurol. 2014; 522:3120–37. [PubMed: 24610730]

Haus DL, Lopez-Velazquez L, Gold EM, Cunningham KM, Perez H, Anderson AJ, Cummings BJ. Transplantation of human neural stem cells restores cognition in an immunodeficient rodent model of traumatic brain injury. Exp Neurol. 2016; 281:1–16. [PubMed: 27079998]

Hayward NM, Immonen R, Tuunanen PI, Ndode-Ekane XE, Grohn O, Pitkanen A. Association of chronic vascular changes with functional outcome after traumatic brain injury in rats. J Neurotrauma. 2010; 27:2203–19. [PubMed: 20839948]

Hayward NM, Tuunanen PI, Immonen R, Ndode-Ekane XE, Pitkanen A, Grohn O. Magnetic resonance imaging of regional hemodynamic and cerebrovascular recovery after lateral fluid-percussion brain injury in rats. J Cereb Blood Flow Metab. 2011; 31:166–77. [PubMed: 20485295]

Hendrich KS, Kochanek PM, Williams DS, Schiding JK, Marion DW, Ho C. Early perfusion after controlled cortical impact in rats: quantification by arterial spin-labeled MRI and the influence of spin-lattice relaxation time heterogeneity. Magn Reson Med. 1999; 42:673–81. [PubMed: 10502755]

Honda M, Ichibayashi R, Yokomuro H, Yoshihara K, Masuda H, Haga D, Seiki Y, Kudoh C, Kishi T. Early Cerebral Circulation Disturbance in Patients Suffering from Severe Traumatic Brain Injury (TBI): A Xenon CT and Perfusion CT Study. Neurol Med Chir (Tokyo). 2016; 56:501–9. [PubMed: 27356957]

Izumi Y, Haida M, Hata T, Isozumi K, Kurita D, Shinohara Y. Distribution of brain oedema in the contralateral hemisphere after cerebral infarction: repeated MRI measurement in the rat. J Clin Neurosci. 2002; 9:289–93. [PubMed: 12093136]

Jiang Q, Qu C, Chopp M, Ding GL, Davarani SP, Helpern JA, Jensen JH, Zhang ZG, Li L, Lu M, Kaplan D, Hu J, Shen Y, Kou Z, Li Q, Wang S, Mahmood A. MRI evaluation of axonal reorganization after bone marrow stromal cell treatment of traumatic brain injury. NMR Biomed. 2011; 24:1119–28. [PubMed: 21432927]

Kaloostian P, Robertson C, Gopinath SP, Stippler M, King CC, Qualls C, Yonas H, Nemoto EM. Outcome prediction within twelve hours after severe traumatic brain injury by quantitative cerebral blood flow. J Neurotrauma. 2012; 29:727–34. [PubMed: 22111910]

Kelly DF, Martin NA, Kordestani R, Counelis G, Hovda DA, Bergsneider M, McBride DQ, Shalmon E, Herman D, Becker DP. Cerebral blood flow as a predictor of outcome following traumatic brain injury. J Neurosurg. 1997; 86:633–41. [PubMed: 9120627]

Kenney K, Amyot F, Haber M, Pronger A, Bogoslovsky T, Moore C, Diaz-Arrastia R. Cerebral Vascular Injury in Traumatic Brain Injury. Exp Neurol. 2016; (275 Pt. 3):353–66.

Kim J, Whyte J, Patel S, Avants B, Europa E, Wang J, Slattery J, Gee JC, Coslett HB, Detre JA. Resting cerebral blood flow alterations in chronic traumatic brain injury: an arterial spin labeling perfusion FMRI study. J Neurotrauma. 2010; 27:1399–411. [PubMed: 20528163]

Korn A, Golan H, Melamed I, Pascual-Marqui R, Friedman A. Focal cortical dysfunction and blood-brain barrier disruption in patients with Postconcussion syndrome. J Clin Neurophysiol. 2005; 22:1–9. [PubMed: 15689708]

Lee RH, Pulin AA, Seo MJ, Kota DJ, Ylostalo J, Larson BL, Semprun-Prieto L, Delafontaine P, Prockop DJ. Intravenous hMSCs improve myocardial infarction in mice because cells embolized in lung are activated to secrete the anti-inflammatory protein TSG-6. Cell Stem Cell. 2009; 5:54–63. [PubMed: 19570514]

Li L, Jiang Q, Zhang L, Ding G, Wang L, Zhang R, Zhang ZG, Li Q, Ewing JR, Kapke A, Lu M, Chopp M. Ischemic cerebral tissue response to subventricular zone cell transplantation measured by iterative self-organizing data analysis technique algorithm. J Cereb Blood Flow Metab. 2006; 26:1366–77. [PubMed: 16511501]

Li L, Jiang Q, Qu CS, Ding GL, Li QJ, Wang SY, Lee JH, Lu M, Mahmood A, Chopp M. Transplantation of marrow stromal cells restores cerebral blood flow and reduces cerebral atrophy in rats with traumatic brain injury: in vivo MRI study. J Neurotrauma. 2011; 28:535–45. [PubMed: 21275806]

Li L, Chopp M, Ding GL, Qu CS, Li QJ, Lu M, Wang S, Nejad-Davarani SP, Mahmood A, Jiang Q. MRI measurement of angiogenesis and the therapeutic effect of acute marrow stromal cell administration on traumatic brain injury. J Cereb Blood Flow Metab. 2012; 32:2023–32. [PubMed: 22781331]

Li L, Chopp M, Ding G, Qu C, Nejad-Davarani SP, Davoodi-Bojd E, Li Q, Mahmood A, Jiang Q. Diffusion-Derived Magnetic Resonance Imaging Measures of Longitudinal Microstructural Remodeling Induced by Marrow Stromal Cell Therapy after Traumatic Brain Injury. J Neurotrauma. 2017; 34:182–191. [PubMed: 26993214]

Li W, Long JA, Watts LT, Jiang Z, Shen Q, Li Y, Duong TQ. A quantitative MRI method for imaging blood-brain barrier leakage in experimental traumatic brain injury. PLoS One. 2014; 9:e114173. [PubMed: 25478693]

Li W, Watts L, Long J, Zhou W, Shen Q, Jiang Z, Li Y, Duong TQ. Spatiotemporal changes in blood-brain barrier permeability, cerebral blood flow, T2 and diffusion following mild traumatic brain injury. Brain Res. 2016; 1646:53–61. [PubMed: 27208495]

Lin Y, Pan Y, Wang M, Huang X, Yin Y, Wang Y, Jia F, Xiong W, Zhang N, Jiang JY. Blood-brain barrier permeability is positively correlated with cerebral microvascular perfusion in the early fluid percussion-injured brain of the rat. Lab Invest. 2012; 92:1623–34. [PubMed: 22964852]

Liu W, Wang B, Wolfowitz R, Yeh PH, Nathan DE, Graner J, Tang H, Pan H, Harper J, Pham D, Oakes TR, French LM, Riedy G. Perfusion deficits in patients with mild traumatic brain injury characterized by dynamic susceptibility contrast MRI. NMR Biomed. 2013; 26:651–63. [PubMed: 23456696]

Long JA, Watts LT, Li W, Shen Q, Muir ER, Huang S, Boggs RC, Suri A, Duong TQ. The effects of perturbed cerebral blood flow and cerebrovascular reactivity on structural MRI and behavioral readouts in mild traumatic brain injury. J Cereb Blood Flow Metab. 2015; 35:1852–61. [PubMed: 26104285]

Luh WM, Wong EC, Bandettini PA, Hyde JS. QUIPSS II with thin-slice TI1 periodic saturation: a method for improving accuracy of quantitative perfusion imaging using pulsed arterial spin labeling. Magn Reson Med. 1999; 41:1246–54. [PubMed: 10371458]

Mahmood A, Lu D, Lu M, Chopp M. Treatment of traumatic brain injury in adult rats with intravenous administration of human bone marrow stromal cells. Neurosurgery. 2003; 53:697–702. discussion 702–3. [PubMed: 12943585]

Mahmood A, Lu D, Qu C, Goussev A, Zhang ZG, Lu C, Chopp M. Treatment of traumatic brain injury in rats with erythropoietin and carbamylated erythropoietin. J Neurosurg. 2007; 107:392–7.

Mahmood A, Qu C, Ning R, Wu H, Goussev A, Xiong Y, Irtenkauf S, Li Y, Chopp M. Treatment of TBI with collagen scaffolds and human marrow stromal cells increases the expression of tissue plasminogen activator. J Neurotrauma. 2011; 28:1199–207. [PubMed: 21355820]

Menge T, Zhao Y, Zhao J, Wataha K, Gerber M, Zhang J, Letourneau P, Redell J, Shen L, Wang J, Peng Z, Xue H, Kozar R, Cox CS Jr, Khakoo AY, Holcomb JB, Dash PK, Pati S. Mesenchymal stem cells regulate blood-brain barrier integrity through TIMP3 release after traumatic brain injury. Sci Transl Med. 2012; 4:161ra150.

Newsome MR, Scheibel RS, Chu Z, Hunter JV, Li X, Wilde EA, Lu H, Wang ZJ, Lin X, Steinberg JL, Vasquez AC, Cook L, Levin HS. The relationship of resting cerebral blood flow and brain activation during a social cognition task in adolescents with chronic moderate to severe traumatic brain injury: a preliminary investigation. Int J Dev Neurosci. 2012; 30:255–66. [PubMed: 22120754]

Opydo-Chanek M. Bone marrow stromal cells in traumatic brain injury (TBI) therapy: true perspective or false hope? Acta Neurobiol Exp (Wars). 2007; 67:187–95. [PubMed: 17691227]

Park E, Bell JD, Siddiq LP, Baker AJ. An analysis of regional microvascular loss and recovery following two grades of fluid percussion trauma: a role for hypoxia-inducible factors in traumatic brain injury. J Cereb Blood Flow Metab. 2009; 29:575–84. [PubMed: 19088740]

Park HJ, Shin JY, Kim HN, Oh SH, Song SK, Lee PH. Mesenchymal stem cells stabilize the blood-brain barrier through regulation of astrocytes. Stem Cell Res Ther. 2015; 6:187. [PubMed: 26420371]

Parr AM, Tator CH, Keating A. Bone marrow-derived mesenchymal stromal cells for the repair of central nervous system injury. Bone Marrow Transplant. 2007; 40:609–19. [PubMed: 17603514]

Pasco A, Lemaire L, Franconi F, Lefur Y, Noury F, Saint-Andre JP, Benoit JP, Cozzone PL, Le Jeune JJ. Perfusional deficit and the dynamics of cerebral edemas in experimental traumatic brain injury using perfusion and diffusion-weighted magnetic resonance imaging. J Neurotrauma. 2007; 24:1321–30. [PubMed: 17711393]

Pati S, Khakoo AY, Zhao J, Jimenez F, Gerber MH, Harting M, Redell JB, Grill R, Matsuo Y, Guha S, Cox CS, Reitz MS, Holcomb JB, Dash PK. Human mesenchymal stem cells inhibit vascular permeability by modulating vascular endothelial cadherin/beta-catenin signaling. Stem Cells Dev. 2011; 20:89–101. [PubMed: 20446815]

Prabhakar H, Sandhu K, Bhagat H, Durga P, Chawla R. Current concepts of optimal cerebral perfusion pressure in traumatic brain injury. J Anaesthesiol Clin Pharmacol. 2014; 30:318–27. [PubMed: 25190937]

Rolfe, A., Sun, D. Brain Neurotrauma: Molecular, Neuropsychological, and Rehabilitation Aspects. Vol. 2015. Taylor & Francis Group, LLC; Boca Raton FL: 2015. Stem Cell Therapy in Brain Trauma: Implications for Repair and Regeneration of Injured Brain in Experimental TBI Models.

Rutland-Brown W, Langlois JA, Thomas KE, Xi YL. Incidence of traumatic brain injury in the United States, 2003. J Head Trauma Rehabil. 2006; 21:544–8. [PubMed: 17122685]

Shlosberg D, Benifla M, Kaufer D, Friedman A. Blood-brain barrier breakdown as a therapeutic target in traumatic brain injury. Nat Rev Neurol. 2010; 6:393–403. [PubMed: 20551947]

Sidaros A, Skimminge A, Liptrot MG, Sidaros K, Engberg AW, Herning M, Paulson OB, Jernigan TL, Rostrup E. Long-term global and regional brain volume changes following severe traumatic brain injury: a longitudinal study with clinical correlates. Neuroimage. 2009; 44:1–8. [PubMed: 18804539]

Stein DM, Hu PF, Brenner M, Sheth KN, Liu KH, Xiong W, Aarabi B, Scalea TM. Brief episodes of intracranial hypertension and cerebral hypoperfusion are associated with poor functional outcome after severe traumatic brain injury. J Trauma. 2011; 71:364–73. discussion 373–4. [PubMed: 21825940]

Su EJ, Fredriksson L, Kanzawa M, Moore S, Folestad E, Stevenson TK, Nilsson I, Sashindranath M, Schielke GP, Warnock M, Ragsdale M, Mann K, Lawrence AL, Medcalf RL, Eriksson U, Murphy GG, Lawrence DA. Imatinib treatment reduces brain injury in a murine model of traumatic brain injury. Front Cell Neurosci. 2015; 9:385. [PubMed: 26500491]

Taguchi A, Sakai C, Soma T, Kasahara Y, Stern DM, Kajimoto K, Ihara M, Daimon T, Yamahara K, Doi K, Kohara N, Nishimura H, Matsuyama T, Naritomi H, Sakai N, Nagatsuka K. Intravenous Autologous Bone Marrow Mononuclear Cell Transplantation for Stroke: Phase1/2a Clinical Trial in a Homogeneous Group of Stroke Patients. Stem Cells Dev. 2015; 24:2207–18. [PubMed: 26176265]

Tang G, Liu Y, Zhang Z, Lu Y, Wang Y, Huang J, Li Y, Chen X, Gu X, Wang Y, Yang GY. Mesenchymal stem cells maintain blood-brain barrier integrity by inhibiting aquaporin-4 upregulation after cerebral ischemia. Stem Cells. 2014; 32:3150–62. [PubMed: 25100404]

Tang H, Sha H, Sun H, Wu X, Xie L, Wang P, Xu C, Larsen C, Zhang HL, Gong Y, Mao Y, Chen X, Zhou L, Feng X, Zhu J. Tracking induced pluripotent stem cells-derived neural stem cells in the central nervous system of rats and monkeys. Cell Reprogram. 2013; 15:435–42. [PubMed: 24020696]

Thal SC, Neuhaus W. The blood-brain barrier as a target in traumatic brain injury treatment. Arch Med Res. 2014; 45:698–710. [PubMed: 25446615]

Thurman DJ, Alverson C, Dunn KA, Guerrero J, Sniezek JE. Traumatic brain injury in the United States: A public health perspective. J Head Trauma Rehabil. 1999; 14:602–15. [PubMed: 10671706]

Tomkins O, Shelef I, Kaizerman I, Eliushin A, Afawi Z, Misk A, Gidon M, Cohen A, Zumsteg D, Friedman A. Blood-brain barrier disruption in post-traumatic epilepsy. J Neurol Neurosurg Psychiatry. 2008; 79:774–7. [PubMed: 17991703]

Villapol S, Byrnes KR, Symes AJ. Temporal dynamics of cerebral blood flow, cortical damage, apoptosis, astrocyte-vasculature interaction and astrogliosis in the pericontusional region after traumatic brain injury. Front Neurol. 2014; 5:82. [PubMed: 24926283]

Wang JY, Bakhadirov K, Devous MD Sr, Abdi H, McColl R, Moore C, Marquez de la Plata CD, Ding K, Whittemore A, Babcock E, Rickbeil T, Dobervich J, Kroll D, Dao B, Mohindra N, Madden CJ, Diaz-Arrastia R. Diffusion tensor tractography of traumatic diffuse axonal injury. Arch Neurol. 2008; 65:619–26. [PubMed: 18474737]

Wei XE, Zhang YZ, Li YH, Li MH, Li WB. Dynamics of rabbit brain edema in focal lesion and perilesion area after traumatic brain injury: a MRI study. J Neurotrauma. 2012; 29:2413–20. [PubMed: 21675826]

Wong EC, Buxton RB, Frank LR. Implementation of quantitative perfusion imaging techniques for functional brain mapping using pulsed arterial spin labeling. NMR Biomed. 1997; 10:237–49. [PubMed: 9430354]

Wong EC, Buxton RB, Frank LR. A theoretical and experimental comparison of continuous and pulsed arterial spin labeling techniques for quantitative perfusion imaging. Magn Reson Med. 1998; 40:348–55. [PubMed: 9727936]

Xiong Y, Qu C, Mahmood A, Liu Z, Ning R, Li Y, Kaplan DL, Schallert T, Chopp M. Delayed transplantation of human marrow stromal cell-seeded scaffolds increases transcallosal neural fiber length, angiogenesis, and hippocampal neuronal survival and improves functional outcome after traumatic brain injury in rats. Brain Res. 2009; 1263:183–91. [PubMed: 19368838]

Xiong Y, Mahmood A, Chopp M. Neurorestorative treatments for traumatic brain injury. Discov Med. 2010; 10:434–42. [PubMed: 21122475]

Yang SH, Gustafson J, Gangidine M, Stepien D, Schuster R, Pritts TA, Goodman MD, Remick DG, Lentsch AB. A murine model of mild traumatic brain injury exhibiting cognitive and motor deficits. J Surg Res. 2013; 184:981–8. [PubMed: 23622728]

Yu Y, Jiang Q, Miao Y, Li J, Bao S, Wang H, Wu C, Wang X, Zhu J, Zhong Y, Haacke EM, Hu J. Quantitative analysis of clinical dynamic contrast-enhanced MR imaging for evaluating treatment response in human breast cancer. Radiology. 2010; 257:47–55. [PubMed: 20713609]

Ziegler D, Cravens G, Poche G, Gandhi R, Tellez M. Use of Transcranial Doppler in Patients with Severe Traumatic Brain Injuries. J Neurotrauma. 2016

Highlights

- Traumatic brain injury results in a diffuse BBB damage and hemodynamic disruption.
- Temporal profiles of Ki and CBF post-TBI in a broad region have been revealed.
- Treatment with hMSCs after TBI expedites the reduction of Ki in the injured brain.
- Treatment with hMSCs after TBI retards the diminution of CBF in the injured brain.
- Earlier cell intervention leads to stronger therapeutic effects on both Ki and CBF.

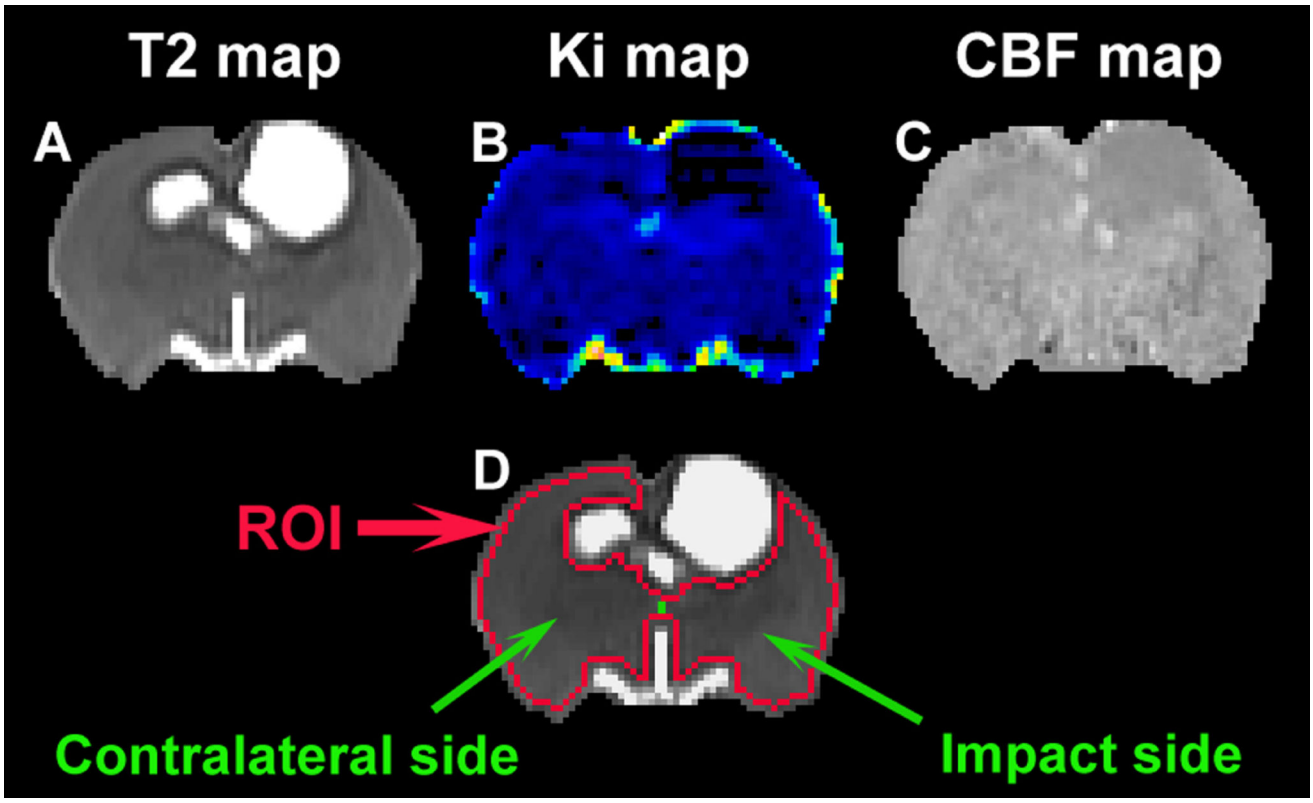

Fig. 1. A representative slice of cell-treated animal showing T2 (A), Ki (B), CBF (C) maps and ROI (D)

TBI-induced disturbance is apparent around the impact site on each of specific maps (A–C). Based on T2 map, the ROI (D, red track) encompassing the normal-appearing brain tissue is created and is divided to two parts (D, green line), impact side and contralateral side (D, indicated by green arrows).

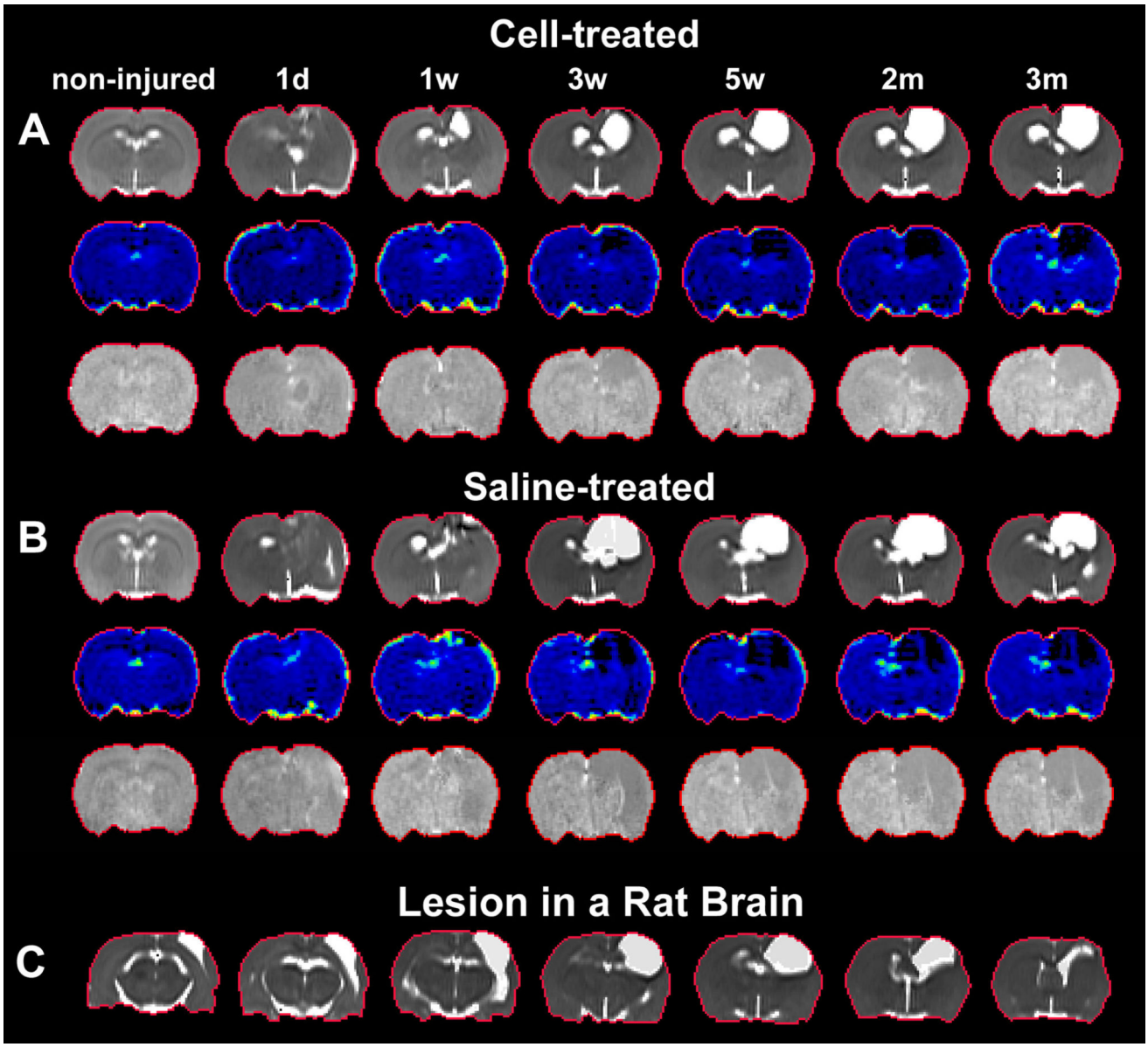

Fig. 2. Dynamic comparison of representative animals with (A) and without (B) cell intervention and a typical lesion in the injured brain (C)

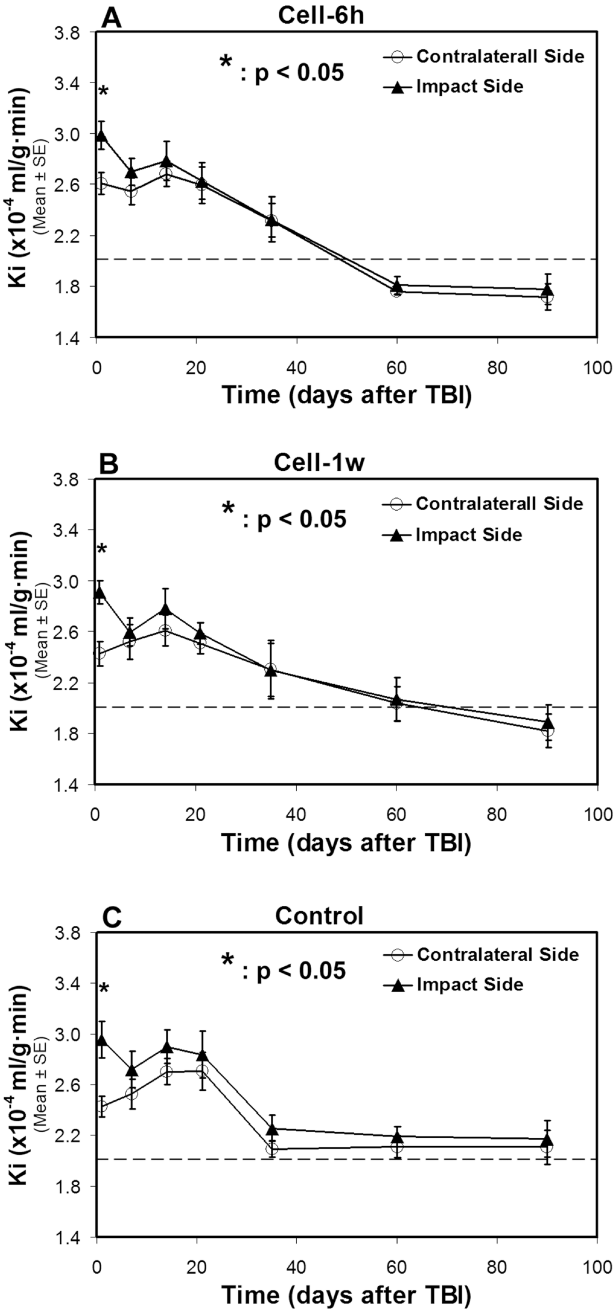

Fig. 3. Changes of Ki in two sides of normal-appearing brain tissue with (A–B) and without (C) cell administration after TBI

A statistical difference in Ki between two sides of the brain is detected at 1-day after TBI for all treatment groups, with a significantly higher Ki value being present in the ipsilateral side than in the contralateral side of the injured brain. After 1-week post-TBI, similar temporal profiles of Ki, however, are found in two sides of the brain without statistical difference for each group, even though each group exhibits a distinct temporal pattern of Ki. The dotted line represents the Ki value in the normal rat brain.

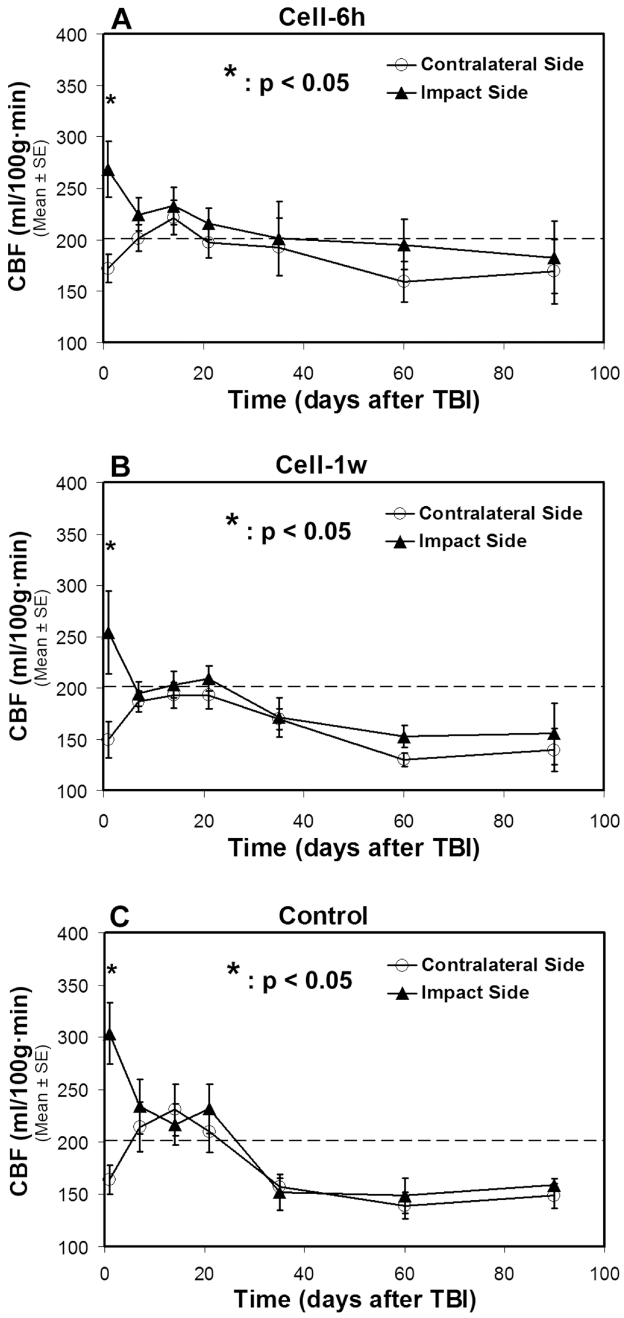

Fig. 4. Changes of CBF in two sides of normal-appearing brain tissue with (A–B) and without (C) cell administration after TBI

A statistical difference in CBF between two sides of the brain is found at 1-day after TBI for all treatment groups, with a significantly increased CBF value being detected in the ipsilateral side than in the contralateral side of the injured brain. After 1-week post-TBI, there is no statistical difference in CBF between two sides of the brain for each group, even though the distinctive features are observed in the temporal profile of CBF for particular treatment group. The dotted line represents the CBF value in the normal rat brain.

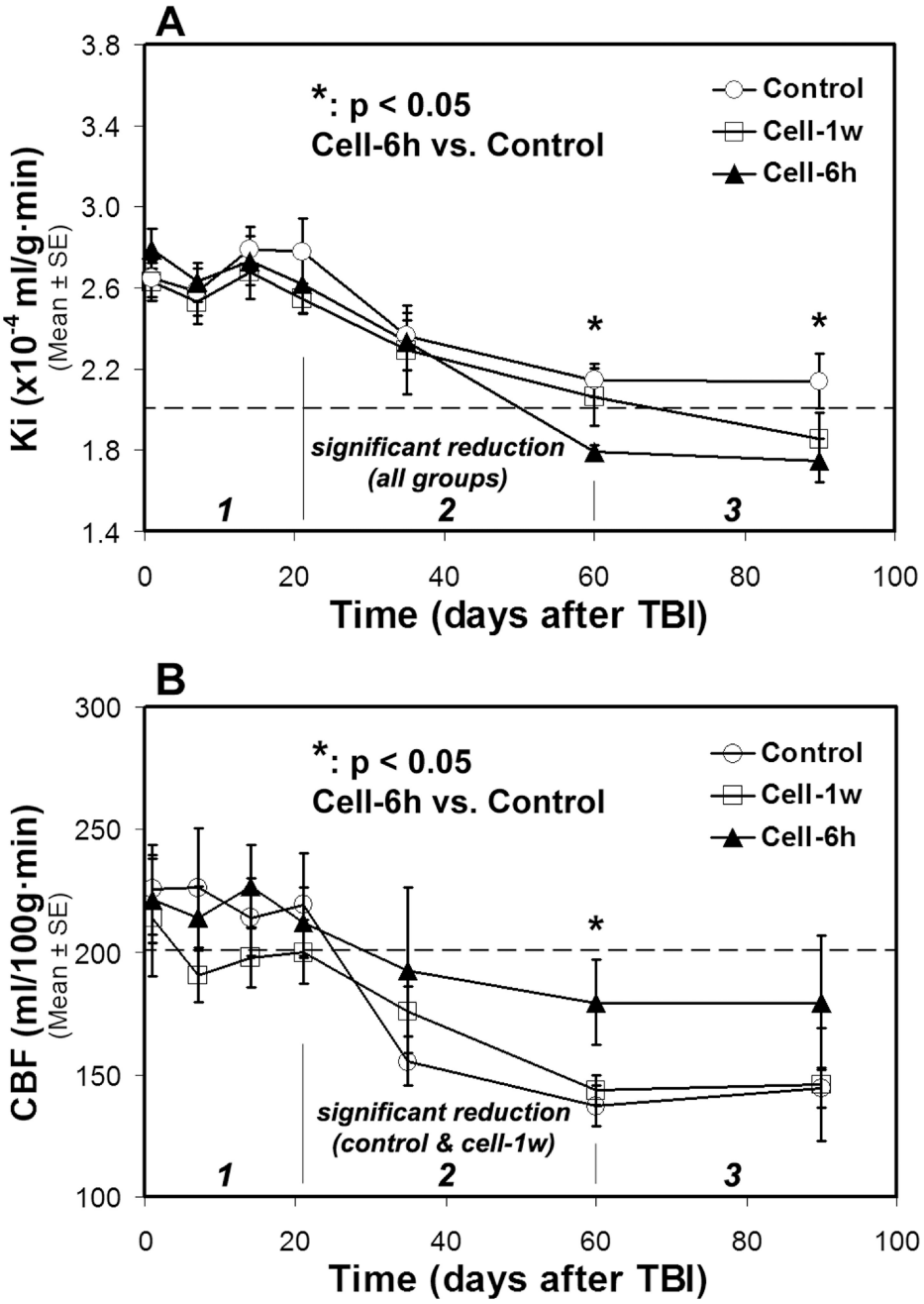

Fig. 5. Changes of Ki (A) and CBF (B) in ROI encompassing both sides of normal-appearing brain tissue

A three-stage evolution pattern of Ki and CBF along with time after TBI was revealed. Both Ki and CBF decrease in stage 2, while these measures fluctuate in stage 1 and tend towards stability in stage 3 for each treatment group. Cell engraftment expedites the reduction of Ki and retards the diminution of CBF in stage 2, resulting in lower Ki and higher CBF values in stage 3 compared to saline administration. The dotted lines represent the Ki and CBF values in the normal rat brain.

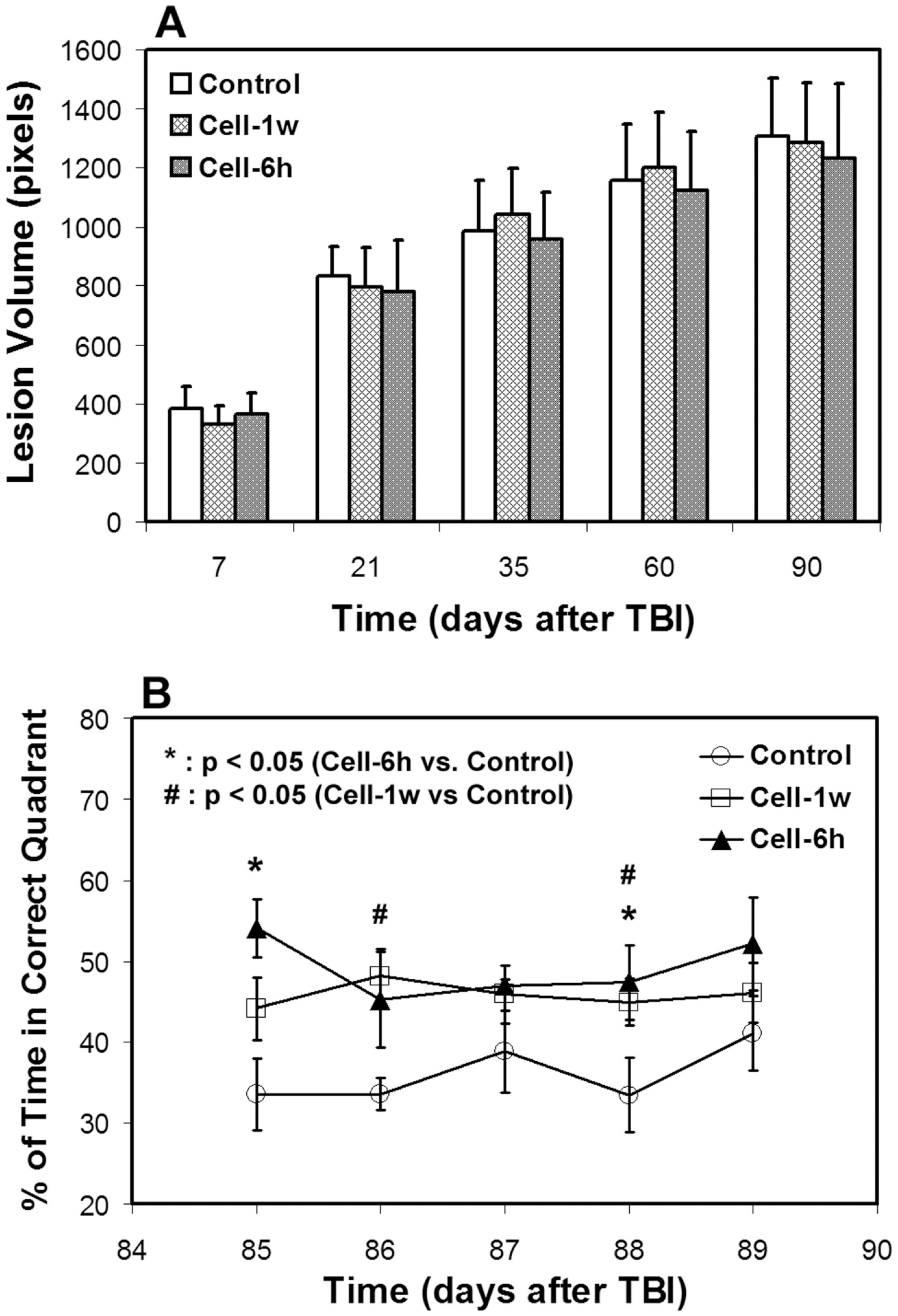

Fig. 6. Lesion volume (A) and water maze result (B)

There was no difference in lesion volume among the treatment groups during the observation period (A). Significantly improved neurological performance was detected in the cell-treated groups compared to the saline-treated group (B).